TRAJECTORY CORRECTION IN THE FERMI@ELETTRA LINAC

S. Di Mitri[#], Sincrotrone Trieste, Trieste, Italy
A. A. Zholents, Lawrence Berkeley National Laboratory, Berkley, CA, 94720, USA.

Abstract

The effect of the static magnetic field errors and misalignment of the magnetic elements and linac modules on the beam trajectory in the Fermi@elettra linac [1] has been studied. Analytical description has been used to guide simulations of the trajectory correction using three different techniques. A control over the residual R_{56} transfer matrix element along the linac lattice has been applied. The importance of the linac structural transverse wake field for a reliable prediction of the bunch centroid dynamics has been demonstrated. Transverse deviations of bunch slices along the electron bunch induced by the wake fields have been calculated.

TRAJECTORY DISTORTION

Table 1shows typical errors used in our study. They include dipole field errors, quadrupole gradient errors, misalignment of magnets, accelerating modules, and Beam Position Monitors (BPMs). We also used trajectory launching errors approximately equal to 2 times of the rms beam sizes at the linac entrance. Electron beam trajectories have been calculated using Elegant [2] tracking code. Few examples of the trajectory distortions caused by errors are shown in Figure 1. The maximum spurious horizontal dispersion seen in these simulations was 2 cm.

Table 1: RMS errors values. Gaussian distribution truncated at 3 sigma is used.

	$\Delta(b_i l)/(b_i l)$ [%]	Δx, Δy [μm]	Δz [μm]	Δθ [mrad]
DIPOLES	0.01	150	200	1
QUADS	0.01	150	200	1
ACC. MODULES	-	300	200	-
BPMs	-	150	200	-
Launching error	Δx, Δy =-300 μm, Δx', Δy'=-50 μrad			

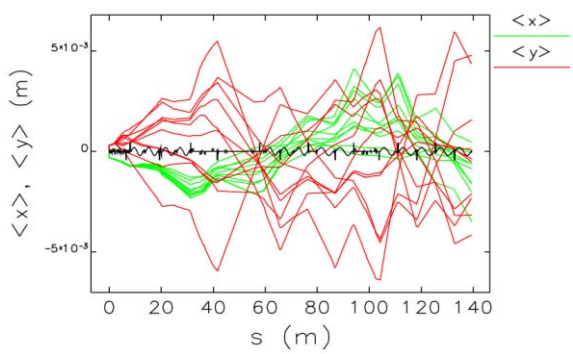

Figure 2: Linac trajectory distortion.

[#]simone.dimitri@elettra.trieste.it

TRAJECTORY CORRECTION

Correction Techniques

Two consecutive BPMs followed by a screen for the characterization of the position, angular divergence and transverse shape of the incoming beam, have been included in the first few meters. The central part of the linac includes 26 horizontal and vertical steerers and 30 BPMs; a quadrupole is between each pair of them. The correction sensitivity is maximized by a separation equal to a quarter of the "effective" betatron wavelength [3]; this reduces to 5 m for quadrupole strength $k = 2$ m^{-2} and magnetic length $l_q = 0.2$ m (typical values in the Fermi linac).

Different codes implement different trajectory correction methods. Mad8.2 [4] foresees several techniques, the faster and most efficient of which is called "lmdif". It minimizes the sum of squares of the constraints – beam centroid position and angular divergence at the BPMs location – by using their derivatives. A typical result for the FERMI linac is shown in Figure 3.

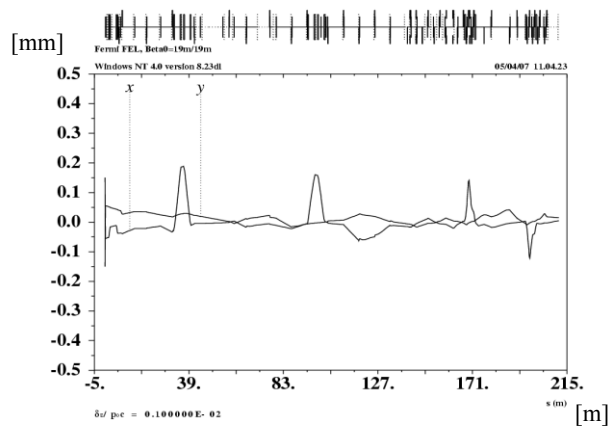

Figure 3: Trajectory correction in the FERMI linac and in the post linac transfer line calculated using Mad8.2 code.

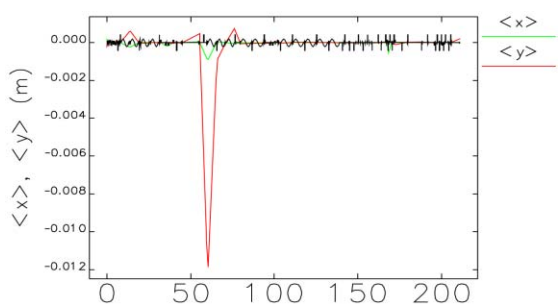

Figure 4: "One-to-one" trajectory correction in the FERMI linac (Elegant code).

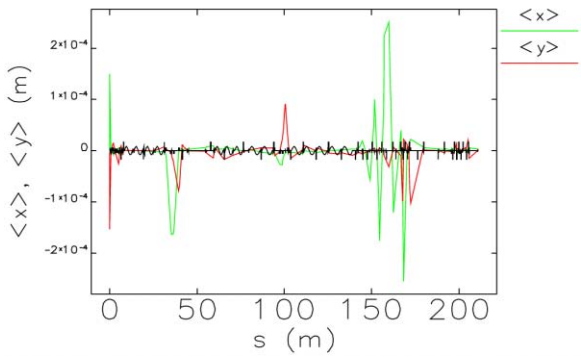

Figure 5: "global" trajectory correction in the FERMI linac and in the post linac transfer line obtained using Elegant code.

Elegant implements "one-to-one" and "global" correction techniques (see, Figure 4 and 5). The first couples each corrector with the BPM immediately downstream; the latter minimizes all the BPM readings by using the trajectory Response Matrix.

COLLECTIVE EFFECTS

Coherent Synchrotron Radiation (CSR) generated in the magnetic chicanes (laser heater, first and second magnetic compressor) induces a variation of the average beam energy which corrupts the achromaticity of the lattice and translates into a trajectory displacement at the chicane exit. Elegant simulations and theoretical evaluations demonstrate that the radiation emission leads to an off-axis trajectory of the order of 100 μm; this is negligible with respect to the trajectory distortion induced by the errors setting listed in Table 1.

The geometric transverse wake fields acting in the accelerating modules are more important than CSR because they modify the particle distribution in the transverse planes and so shift the position of the centre of mass within the bunch. As a result, the BPM readings contribute to center the bunch core on the reference axis of the line, while the bunch head and tail may remain off-axis by a certain amount caused by the Single Bunch Beam Break Up (SBBU) instability [5]. Simulations show that the SBBU instability has an important effect on the trajectory distortion and correction.

Global Trajectory Correction

Global trajectory correction implemented in Elegant limits corrector's strength to angular kicks < 2 mrad (the largest ones are located mainly at a low energy and in the last linac section, i.e. Linac4, where trajectory bumps described in the next section are used.. The maximum spurious dispersion is now 1 cm in both planes. The off-axis trajectory is contained within approximately 350 μm rms in the transverse planes, over the whole linac length and for a statistic sample of 120 runs (see, Figure 5).

Particle tracking shows that correcting trajectory is not enough for a suppression of the SBBU instability bending the electron beam into a characteristic "banana" shape. Nevertheless, a more efficient correction scheme helps in reducing the bunch head-tail excursion so that weaker and less invasive local trajectory bumps can be used to reduce the banana shape. Figure 6 compares the head-tail lateral displacement obtained at the linac end for an old and partially optimized correction scheme and that for the current optimized scheme: the rms banana shape is reduced by a factor 2 in the horizontal plane.

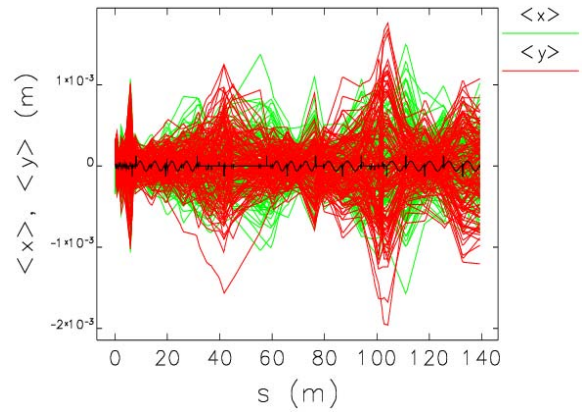

Figure 6: Horizontal and vertical trajectories after correction. 120 errors setting have been based on the tolerances given in Table 1.

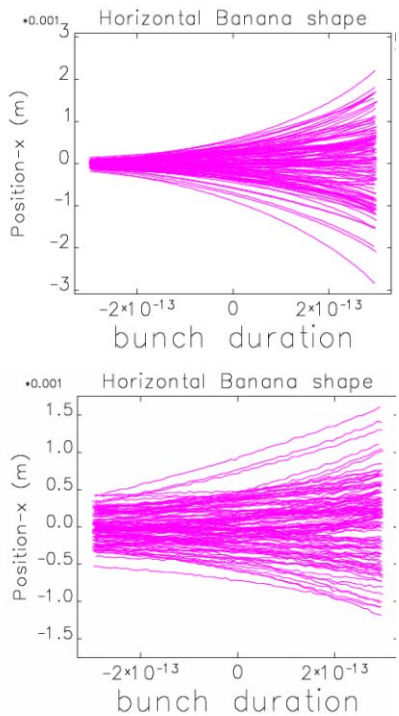

Figure 7: Horizontal banana shapes (slice transverse coordinate vs. bunch duration) at the end of the linac lattice with the old (top) and current (bottom) correction scheme; bunch head is for negative time coordinates.

Local Trajectory Bumps

Local trajectory bumps (see, Figure 7) are needed to find the golden trajectory for which the angular kicks provided by the transverse wake field compensate each other and finally a reduced banana shape is obtained (see, Figure 8)

[5]. Figure 7 shows the trajectory correction with bumps applied in the horizontal and vertical plane in the region of Linac4; here, the trajectory still shows reasonable off-axis excursions. The bumps have been performed by using 6 steerers and 6 BPMs distributed along Linac4; the maximum variation of the steerer strengths with respect to the nominal set up is only about 0.2 mrad.

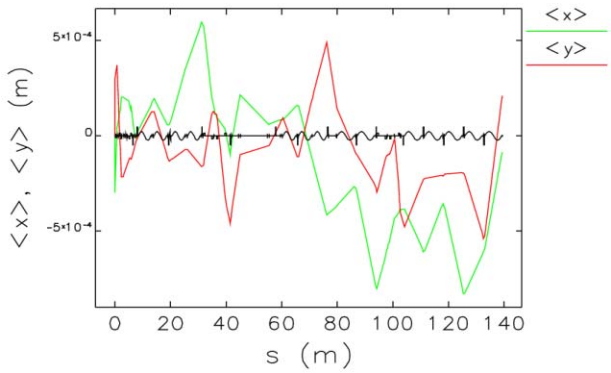

Figure 8: corrected trajectory along the FERMI linac with local bumps applied along the last accelerating modules to suppress the SBBU instability.

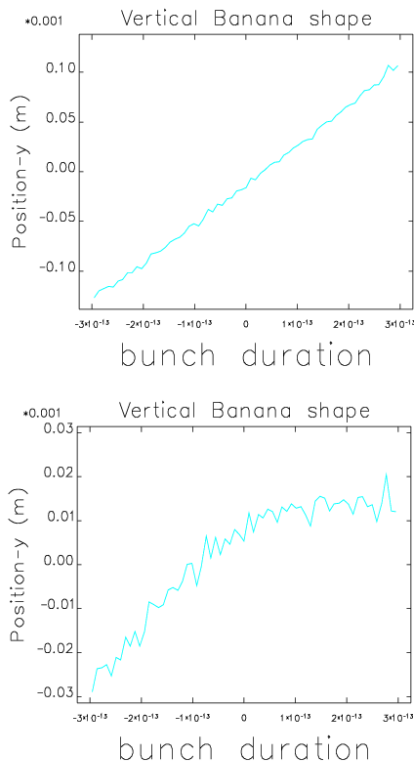

Figure 9: vertical banana shape (slice transverse coordinate vs. bunch duration) at the linac end. After the bumps have been applied (see, Figure 7), the ratio between the head-tail displacement and the rms beam size passes from 4.1 to 0.3 for the horizontal plane and from 2.5 (top plot) to 0.6 (bottom plot) for the vertical plane.

RESIDUAL DISPERSION

The R_{56} transfer matrix element of a transport line can be analytically estimated as follows:

$$R_{56} = \int \frac{D(s)}{\rho(s)} ds \sim \frac{D}{\rho} l$$

where $D(s)$ is the dispersion function in the presence of a local bending radius $\rho(s)$ over a path length l. R_{56} can convert energy modulations into current modulations. This effect in turn degrades the Free Electron Laser (FEL) performance [6]. For 1 mm trajectory offset in the quadrupole and electron beam energy larger than 100 MeV we estimate the effective bending radius of 500 m. Similarly, we estimate the bending radius of corrector magnet causing 0.5 mrad trajectory kick to be 150 m. Thus, the average value of the residual dispersion function for the corrected trajectory is larger in the vertical plane than in the horizontal and it is about 5 mm. Assuming typical values for the magnet strengths one obtains $R_{56} \approx 2.0$ μm for the quadrupole and $R_{56} \approx 2.5$ μm for the steerer. Even in the case of a maximum dispersion $D_y = 1$ cm and a maximum quadrupole strength of $k = 6$ m^{-2}, the result is only $R_{56} \approx 10$μm. If the magnets' contributions would unrealistically sum with the same sign over all the 20 quadrupoles and 26 steerers of the FERMI linac, the residual R_{56} can reach only a few 100's μm, as maximum. As a conclusion, local variations of R_{56} along the linac are of the order of some microns. The variation of R_{56} over the whole linac can reach 100's microns in a very pessimistic scenario. Thus, the effect of microbunching induced by the residual R_{56} in the linac can be neglected.

REFERENCES

[1] S. Di Mitri, ST/M–07/01 (2007).
[2] M. Borland, APS LS-287 (2000).
[3] P. J. Bryant, Beam Transfer Lines, CERN 94-01, Vol.I
[4] H. Grote, F. C. Iselin, CERN/SL/90-13 (AP)
[5] P. Craievich, S. Di Mitri, Emittance growth due to short-range transverse wakefields in the FERMI linac, Proc. FEL 2005, SLAC, California, USA (2005).
[6] W. Fawley, G. Penn, ST/F-TN-06/07 (2006).

ACKNOWLEDGEMENT

The author thanks M. Borland, G. Penco, S. Tazzari, and R. Wells for support and useful discussions.

This work was supported in part by the Italian Ministry of University and Research under grants FIRB-RBAP045JF2 and FIRB-RBAP06AWK3.